IOVS Papers in Press. Published on June 26, 2012 as Manuscript iovs.12-9583

Corneal biomechanical properties from two-dimensional corneal flap extensiometry: application to UV-Riboflavin cross-linking

Sabine Kling[1,2], Harilaos Ginis[2], Susana Marcos[1]

[1] Instituto de Óptica "Daza de Valdés", Consejo Superior de Investigaciones Científicas, Madrid

[2] Institute of Vision and Optics, University of Crete, Heraklion

Word count: 3012

Financial support / Funding:

EURYI 05-102-ES, European Young Investigator Award; Spanish Government FIS2008-02065 and FIS2011- 25637 grants to SM, and FPI Predoctoral Fellowship to SK.

Abstract:

PURPOSE: Corneal biomechanical properties are usually measured by strip-extensiometry or inflation-methods. We developed a 2D-flap extensiometry technique, combining the advantages of both methods, and applied it to measure the effect of UV-Riboflavin-cross-linking (CXL).

METHODS: Corneal-flaps (13 pig / 8 rabbit) from the de-epithelialized anterior stroma (96 µm) were mounted on a custom chamber, consisting of a BK-7 lens, a reflective retina and two reservoirs (filled with Riboflavin and silicon-oil). Stretching the corneal flap during 5 pressure in/decrease cycles (0-30mmHg) changed the refractive power of the system, whose Zernike aberrations were monitored with a ray-tracing aberrometer. Porcine flaps were used to test the system. Rabbits were treated

with corneal cross-linking (CXL) unilaterally in-vivo following standard clinical procedures. Flaps were measured 1-month post-operatively. An analytical model allowed estimating Young Modulus from the change in surface (strain) and pressure (stress). Confocal microscopy examination was performed before and at different times after CXL.

RESULTS: Flap curvature changed with increased function of intraocular pressure in pig flaps (23.4 $\cdot 10^{-3}$ D/mmHg). In rabbit flaps curvature changed significantly less in 1-month post-CXL ($p=0.026$) than in untreated corneas (17.0 vs 6.36 mD/mmHg). Young's modulus was 2.29MPa in porcine corneas, 1.98 MPa in untreated rabbit corneas and 4.83MPa in 1-month post-CXL rabbit corneas. At the same time highly reflective structures were observed in the rabbit mid-stroma after treatment.

CONCLUSIONS: 2D-flap-extensiometry allows estimating corneal elasticity in-vitro. The measurements are spatially resolved in depth, minimize the effects of corneal hydration and preserve the integrity of the cornea. The method proved the efficacy of CXL in increasing corneal rigidity after 1-month in rabbits.

Introduction:

Understanding corneal biomechanical properties is critical to model the biomechanical response of pathological corneal tissue (i.e. keratoconus, a progressive corneal disease that debilitates corneal tissue) and to increase the predictability of surgical outcomes or treatments (i.e. intrastromal ring segments, corneal cross-linking or incisional surgery). Various methods have been used in the past to estimate the corneal modulus of elasticity (Young modulus). The most widespread applied method is strip extensiometry,[1,2,3,4] followed by corneal button inflation[5,6] and whole-globe inflation.[4,7,8,9,10] In these techniques a load is applied (typically along one axis, in strip extensiometry - or radially by increasing intraocular pressure, in inflation techniques). The strain upon the applied stress is measured from the lateral elongation, axial apex displacement,[4] shift of mercury droplets attached

on the corneal surface,[5,7] or from changes in the corneal radius of curvature.[10,11] A new technique to estimate the corneal biomechanical properties, by measuring the corneal deformation upon air-puff applanation, has been recently suggested.[12,13] In all in-vitro biomechanical measurements, corneal hydration plays a role as it affects the tissue's mechanical response.[14] Also different medical solutions alter the corneal hydration and thus the biomechanical properties of the tissue[15] (Kling S., IOVS, 2010, Corneal Biomechanical Response to Intraocular Pressure Changes From Scheimpflug and Anterior Segment OCT, ARVO E-Abstract, 4628/D750). UV-riboflavin cross-linking (CXL) is an increasingly used technique for the treatment of keratoconus, which aims at stiffening the corneal tissue. The increase in corneal rigidity gained with this treatment is assumed to result from the reaction of the photosensitizer (riboflavin) with UV light, which creates radicals that induce additional cross-links between collagen fibrils, probably interhelically, intrahelically and intermicrofibrillary.[15,16] Strip extensiometry stress-strain experiments showed an increase in corneal rigidity immediately and at several months post CXL in human[2], porcine[2] and rabbit[1] corneas. Also whole-globe inflation experiments showed an immediate increase in corneal rigidity in eyes in-vitro after CXL.[11] The biomechanical response estimated from the previous methods may be affected by the corneal shape (geometry), thickness, hydration state (in vitro) and intraocular pressure (in vivo). In this study we developed a new two-dimensional stress-strain system that allows maintaining the original stress distribution along the corneal flap, while guaranteeing that corneal hydration is equal for all samples. This allows an accurate comparison between individual flaps of a certain layer, as well as a precise analysis of the treatment effects on a few corneal layers. To prove its application we evaluated the change in corneal rigidity following CXL treatment in rabbits.

Methods:

Corneal flaps were mounted in a chamber connected to a pressure system that applied the force to stretch flaps of porcine and rabbit corneas. The flap deformation was monitored with a ray-tracing aberrometer. Rabbit flaps were treated with CXL in-vivo. An analytical model was applied to estimate the tissue elasticity in non-treated corneas and after CXL.

FLAP HOLDER

A custom flap holder (Figure 1) was constructed for two-dimensional stretching of a corneal flap. The holder consisted of two chambers separated by the flap: Chamber 1 was filled with riboflavin-dextran, permitting diffusion of the photosensitizer into the flap in both conditions (non treated, one month after CXL). The chamber was connected to a pressure-system in order to apply a normal surface load onto the flap. Chamber 2 was filled with Oxane 1300 Silicon-Oil (Bausch&Lomb) in order to preserve corneal hydration and because of its high refractive index (1.5). This chamber was left open to provide atmospheric pressure independent of pressure in chamber 1. The dextran in the riboflavin solution in Chamber 1 regulated the flap's hydration while the silicon-oil prevented water evaporation. Under these conditions (ambient temperature, 25ºC) flap hydration was maintained constant throughout treatment and measurements. The size of the opening between chambers where the flap was mounted had a diameter of 6 mm.

PRESSURE SYSTEM

Pressure was modified infusing saline solution in chamber 1 by an automatic pumping system, consisting of a syringe mounted on a custom-built motorized stage. A pressure sensor (SSCM3175GA, Sensortechnics, Germany) was used in combination with a custom LabView routine to monitor the pressure difference between Chambers 1 and 2.

EYES AND FLAP PREPARATION

In-vitro experiments were performed in order to measure the elasticity of corneal flaps and to investigate the effect of changes in rigidity induced by CXL. Measurements were performed on fresh enucleated porcine eyes (non-treated), as well as on New Zealand rabbit eyes (non-treated and 1-month post in-vivo-CXL). Measurements in porcine eyes allowed establishing the technique, while measurements in rabbit eyes allowed evaluating the CXL treatment. Porcine eyes were obtained

from a local slaughterhouse and used within 24 hours. Rabbits were obtained from a certified farm at the age of 3 months (approx. 2 kg weight).

After performing CXL treatment in the left eye, the rabbits were housed in animal facilities where they were cared. A total of 13 porcine eyes and 8 rabbit eyes were tested. The protocols adhered to the ARVO guidelines for animal research and had been approved by the Institutional Review Board.

In porcine eyes in vitro, first the epithelium was removed with a hockey epithelium removal knife and 20% Dextran (Sigma-Aldrich D8821) solution was applied for 40 minutes. Then the intraocular pressure was adjusted to physiologic value (15 mmHg). A flap was cut with a mechanical Carriazo-Pendular microkeratom (Schwind, Germany) and mounted on the custom holder. Ultrasonic pachymetry was performed for the intact eye and for the corneal bed after cutting the flap, in order to estimate the thickness of the removed flap. The extensiometry measurement was conducted in the untreated flap. Riboflavin-Dextran solution was constantly supplied by Chamber 1 from the moment on when the flap was mounted within the system.

Rabbits were anaesthetized using 1ml Ketamine hydrochloride 10% + 2ml Xylazine 2%. CXL was performed following standard clinical conditions (first 30 minutes of riboflavin instillation, followed by 30 minutes 370 nm UV-light exposure (Compact LED Area Light, Edmund Optics) of 3 mW/cm^2, while continuing riboflavin instillation every 3 minutes. Left eyes were treated and right eyes were left untreated for control. Rabbits were euthanized one month after treatment. Corneal flaps were excised immediately after animal sacrifice, mounted on the flap holder and the extensiometry measurement was done.

Rabbit eyes were examined with a confocal light microscope (HRT, Heidelberg Engineering, Heidelberg) at different times: before treatment, immediately after CXL, one day after CXL and one month after CXL.

EXTENSIOMETRY

Measurements were conducted for a series of pressures, for each flap and condition. Initially, the pressure in Chamber 1 was set equal to pressure in Chamber 2 (1013hPa). Then, one preconditioning

cycle was performed up to the pressure of 35 mmHg. Pressure was increased up to 30 mmHg, and then decreased, in about 5 mmHg steps. After preconditioning, ray-tracing measurements were performed for two inflation-deflation cycles.

RAY TRACING MEASUREMENTS

The geometry of the flap was assessed using ray tracing (iTrace, Tracey Technologies Corp, Houston, USA) at each pressure step. Flaps were mounted in the holder and the system was placed as an artificial eye in front of the iTrace for aberrometry measurements (Figure 2). The measurement wavelength was 670 µm. Zernike coefficients (up to the 7^{th} order) were obtained for a pupil diameter of 2.5mm, and the low order terms (defocus and astigmatism) were used for analysis. Changes in the low order aberrations are related to changes in the curvature and astigmatism of the flap surface. Ray tracing measurements were obtained during two inflation cycles for each flap and condition, which in total took about 20 minutes. Measurements were performed in approximately 5mmHg pressure steps.

DATA ANALYSIS

The amount of defocus in the artificial eye is related to the stretching of the corneal flap. The higher the pressure in Chamber 1, the more curved the flap and the higher the change of the system's refractive power. Due to small deformations produced by the applied pressures, it can be assumed that the flap is deformed spherically. This approximation is further justified as we selected a central portion of the flap for measurement and analysis. Zernike coefficients Z_2^0 (defocus term) and Z_2^2 / Z_2^{-2} (astigmatism at 45° / 90° terms) were analyzed. The defocus term was used to calculate the surface area of the flap as a function of pressure: $A_{flap}(p) = \int_0^{r_{flap}} Z_2^0(p) \cdot \sqrt{3} \cdot (2r^2 - 1)\, dr$ (eq. 1) where A_{flap} is the surface area, p is pressure in Chamber 1 and r the distance from the center of the optical axis.

Then, an analytical model was applied to obtain stress $\sigma = p_{chamber1} \cdot \frac{A_{flap}}{th \cdot 2r_{flap}}$ (eq.2) and strain $\varepsilon = \sqrt{\frac{\Delta A_{flap}}{A_{flap_0}}}$ (eq.3) from changes in the flap area, where *th* stands for thickness, *σ* for stress and *ε* for strain. Stress is a measure of the amount of force acting on the cross-sectional area, and strain represents the relative expansion of the original flap area. The absolute pressure variation, and hence the applied force stretching the flap, was sufficiently small, so that elastic deformation only could be assumed. A linear fit was adjusted to the stress-strain relation in order to obtain the corresponding Young's modulus: $E = \frac{\Delta\sigma}{\Delta\varepsilon}$ (eq.4)

The Zernike terms Z_2^2 and Z_2^{-2} were used in order to calculate J_0 and J_{45} following the power vector notation. The calculated astigmatism was analyzed as a function of pressure increase. Absolute differences in the astigmatism between CXL and non-treated flaps were investigated. A students t-test (two sample equal variance, two tailed) was applied to test the statistical differences in the flap shapes across conditions between non-treated and CXL.

Results:

FLAP PACHYMETRIC AND MICROSCOPIC OBSERVATIONS

Corneal flap thickness was 98±21µm in porcine and 96±14µm in rabbit corneas. After manual excision of the hinge, a 6-mm circular portion of the flap was mounted and measured. In compliance with other studies on confocal microscopy[17] we observed highly reflective structures in the rabbit mid-stroma one month after CXL (see Figure 3). Interestingly, these structures could not be observed immediately after, or one day after CXL.

DEFOCUS ABERRATION

Figure 4 shows the change in the defocus term from the Zernike polynomial expansion as a function of pressure in chamber 1 from porcine (4A) and rabbit (4B) flaps. Black symbols represent the control measurement, while white symbols stand for the cross-linked condition. Diamonds stand for increasing pressure and circles for decreasing pressure. Data of the three conditions are the average across 13 porcine corneas, 4 non-treated rabbit corneas, and 4 cross-linked rabbit corneas, respectively. Standard deviations are plotted as error bars in Figure 4. Defocus increased linearly with increasing pressure in all conditions. Trend lines to the average of non-treated (bold) and CXL (thin) data show a positive slope. The lower the slope, the smaller the deformation and the stiffer the corneal flap. The slope in porcine flaps was $23.4 \cdot 10^{-3}$ D/mmHg. In rabbit eyes the slope in the non-treated cornea ($17.0 \cdot 10^{-3}$ D/mmHg) was significantly steeper ($p= 0.105$) than the cross-linked corneas ($6.36 \cdot 10^{-3}$ D/mmHg), consistently with an increase in corneal rigidity after CXL. Variability across samples was 0.22 D in porcine flaps, 0.10 D in non-treated rabbit flaps and 0.08 D in CXL rabbit flaps.

In certain conditions, the flap geometry did not recover its original state after pressure variation, showing a hysteresis. This can be seen by the differences in refractive power at the same pressure in the increasing and decreasing pressure sequences. Porcine corneas did not show this effect ($p=0.338$). However in rabbit corneas, there was a significant shift in defocus (control: $p=0.032$ / CXL: $p=0.007$) after the pressure increased/decrease cycle: 0.19 D in control flaps and 0.39 D in CXL flaps (at 0 mmHg pressure). Actually after CXL the refraction hardly changed with pressure decrease, indicating a permanent plastic deformation. But the small sample size in rabbits might limit the impact of this finding.

ASTIGMATIC ABERRATION

Mean astigmatism was modest, both, in porcine flaps (0.55 D) and in rabbit flaps (0.74 D in non-treated, 0.34 D in CXL), and did not change significantly with pressure variation. In rabbit flaps a small decrease was observed after CXL.

YOUNG'S MODULUS

Young's moduli were calculated for the different conditions. The average Young modulus in porcine flaps was 2.29±1.63MPa. The average Young´s modulus of rabbit flaps was 1.98±0.40 MPa and increased significantly (p=0.003) one month after in-vivo CXL (4.83±1.32 MPa). Figure 5 shows the stress-strain diagram, calculated from average experimental data and equations for stress (eq.2) and strain (eq.3). Average data from the loading and unloading cycle were used to calculate the slopes, which represent Young's modulus according to equation 4.

Discussion:

We present a 2D-flap extensiometry technique, which allows measuring corneal elasticity parameters, minimizing the effects associated with corneal hydration, among others. This method has proved sensitive to detect differences across conditions, and could be used to investigate corneal biomechanical properties at different corneal depths. While in the current study we used a mechanical microkeratome (which limited the thickness accuracy to which the flaps could be cut), the use of a femtosecond laser would allow excising flaps of more resolved thickness and at different depth positions. The method could be used to assess biomechanical properties of different corneal layers (i.e. anterior and posterior stroma). This information is valuable to accurately represent the corneal biomechanical response by spatially resolved finite element models.

We evaluated the potential of the technique on corneal flaps from a porcine model, and investigated the biomechanical changes in the cornea 1-month after CXL in rabbit eyes. The estimated values of Young´s moduli (porcine flap: 2.29 MPa, rabbit flap: 1.98 MPa) fall within the ranges reported in literature, although those vary over more than two orders of magnitude depending on the study.[1,2,8,13,19,5,6,18,21] As a reference, in-vitro strip extensiometry experiments estimated a Young´s modulus of 11.1 MPa for rabbit corneas and of 1.5MPa for porcine corneas.[1,2] An in-vitro button inflation study reported a Young's modulus of 2.87 - 19.5MPa for the human cornea,[8] and a recent study using in-vitro whole globe inflation in porcine eyes reported a Young´s modulus of 1.11MPa (Kling S., IOVS, 2010, Corneal Biomechanical Response to Intraocular Pressure Changes From

Scheimpflug and Anterior Segment OCT, ARVO E-Abstract, 4628/D750). Ultrasound measurements on in-vitro human corneas provided a value of 5.3MPa,[20] and an in-vivo approach based on the deformation with applanation tonometry 0.29MPa in humans[22]. The large differences across reports of Young's modulus likely arise from the different working principles of the techniques, and the hydration condition in which corneal tissue is measured. The Young´s modulus in porcine eyes measured in this study agree well with extensiometry reports by Wollensak et al[2] and inflation models by Kling et al.[11] It is likely that the higher elasticity values found for the flap compared to the Young´s modulus of the entire cornea arise from the fact that only the most anterior layer of the corneal stroma was used in the flap study, as the anterior stroma has been reported to be stiffer than the posterior cornea.[23]

The proposed 2D-flap extensiometry technique reduces the variability by controlling the flap thickness, avoids a major role of hydration and allows a better spatially resolved analysis. The technique therefore combines several advantages from previous methods. First, it guarantees a very similar distribution of the acting force (pressure) to the in-vivo condition, similar to button or whole-globe inflation. As flaps are cut in a predefined thickness, the variation across specimens decreases. Second, the rigid circular fixation of the flap allows an accurate analysis of the corneal expansion, similarly to strip-extensiometry, but preserving a more realistic geometry and the actual orientation of the collagen fibers.

The increase in corneal stiffness that we found after CXL in rabbits (x 2.43) is consistent with the literature. Previous studies reported an increase of corneal stiffness by a factor of 1.58 - 1.8 (in pigs), by 4.5 (in humans) and by 1.6 (in rabbits).[11,1,2] Again, the slightly higher factor can be explained because the flaps were cut on the anterior stroma.. A study of the long-term effects of CXL in rabbits (measured before and immediately after, 3 and 8 months after CXL) showed a high stability in the post-CXL corneal stiffness (a constant pre/post Young modulus ratio over time, by 1.6).[1] Although there are studies reporting an immediate effect of CXL,[2,11] we suggest that apart from this, processes happening at the tissue level (e.g. wound healing) could contribute to the increase in

corneal rigidity after CXL, as structural changes (highly reflective structures, Figure 3) were observed to appear simultaneously with an increase in corneal rigidity.

In a previous study in porcine eyes in vitro[11] we showed stronger stiffening effects of CXL in the horizontal than in the vertical direction. In the current study a slight reduction of corneal astigmatism with CXL was observed in rabbits, which has also been reported clinically in patients.[22]

As a side effect, we observed that porcine corneal flaps did not show differences in the variation of the geometry with increased/decreased pressure, whereas in rabbit flaps a hysteresis was apparent.

The current study on cornel flaps suggests that the spatially resolved analysis (in this case in thin corneal layers) of the processes occurring in CXL, may give insights into the understanding of its mechanisms. The use of new techniques (such as second harmonic microscopy[24]) that allow visualizing collagen at its structural level in combination with the presented 2D-flap approach may lead to interesting advances in the future.

Acknowledgement:

We thank Creta farm S.A. for providing us with enucleated porcine eyes, G. Kontadakis, N. Kariotakis and A. Papadiamantis for technical assistance.

References:

(1) Wollensak G., Iomdina E., Long-term biomechanical properties of rabbit cornea after photodynamic collagen crosslinking, Acta Ophthalmologica, 2009, 87(1): 48-51

(2) Wollensak G. Spoerl E., Seiler T., Stress-strain measurements of human and porcine corneas after riboflavin-ultraviolet-A-induced cross-linking, J Cataract Refrat Surg, 2003, 29: 1780-1785

283 (3) Elsheikh A., Kassem W., W. Jones S., Strain-rate sensitivity of porcine and ovine corneas, Acta of
284 Bioengineering and Biomechanics, 2011, 13(2): 25-36

285 (4) Elsheikh A., Anderson K., Comparative study of corneal strip extensometry and inflation tests, J R
286 Soc Interface, 2005, 2(3): 177-185

287 (5) Boyce B.L., Grazier J.M., Jones R.E., Nguyen T.D., Full-field deformation of bovine cornea under
288 constrained inflation conditions, Biomaterials, 2008, 29(28): 3896-3904

289 (6) Knox Cartwright N.E., Tyrer J.R., Marshall J., Age-Related Differences in the Elasticity of Human
290 Cornea, Invest Invest Ophthalm Vis Sci, 2011, 52(7): 4324-432936

291 (7) Jue B., Maurice D.M., The mechanical properties of the rabbit and human cornea, J Biomech,
292 1986, 19: 847-853

293 (8) Hjortdal J.O., Reginoal elastic performance of the human cornea, J. Biomechanics, 1996, 29(7):
294 931-942

295 (9) Litwiller D.V., Lee S.J., Kolipaka A., Mariappan Y.K., Glaser K.J., Pulido J.S., Ehman R.L., MR
296 elastography of the ex vivo bovine globe, Journal of Magnetic Resonance Imaging, 2010, 32(1): 44-51

297 (10) Pierscionek B.K., Asejczyk-Widlicka M., Schachar R.A., The effect of changing intraocular pressure
298 on the corneal and sclera curvatures in the fresh porcine eye, Br J Ophthalmol, 2007, 91: 801-803

299 (11) Kling S., Remón L., Pérez-Escudero A., Merayo-Lloves J., Marcos S., Corneal biomechanical
300 changes after collagen cross-linking from porcine eye inflation experiments, Invest Ophthal Vis Sci,
301 2010, 51(8): 3961-3968

302 (12) Dorronsoro C., Pascual D., Pérez-Merino P., Kling S., Marcos S., Dynamic OCT measurement of
303 corneal deformation by an air puff in normal and cross-linked corneas, Biomed Opt Exp, 2012, 3(3):
304 473-487

305 (13) Hamilton K.E., Pye D.C., Young´s modulus in normal corneas and the effect on applanation
306 tonometry, Hamilton K.E., Pye D.C., Optom Vis Sci, 2008, 85: 445-450

307 (14) Hjortdal J., Extensibility of the normo hydrated human cornea, Acta Opthalmologica, 1995,
308 73(1): 12-17

309 (15) Abad J.C., Panesso J.L., Corneal collagen cross-linking induced by UVA and riboflavin, Techniques
310 in Ophthalmology, 2008, 6(1): 8-12

311 (16) Wollensak G., Wilsch M., Spoerl E., Seiler T., Collagen fiber diameter in the rabbit cornea after
312 collagen crosslinking by riboflavin/UVA, Cornea, 2004, 23(5): 503-507

313 (17) Guthoff R.F., Zhivov A., Stach O., In vivo confocal microscopy, an inner vision of the cornea – a
314 major review, Clinical and Experimental Ophthalmology, 2009, 37: 100-117

315 (18) Kohlhaas M., Spoerl E., Schilde G., Unger G., Wittig C., Pillunat L.E., Biomechanical evidence of
316 the distribution of cross-links in corneas treated with riboflavin and ultraviolet A light, J Cataract
317 Refract Surg, 2006, 32: 279-283

318 (19) Hjortdal J., Koch Jensen P., In vitro measurement of corneal strain, thickness and curvature using
319 digital image processing, Acta Opthalmologica, 1995, 73: 5-11

320 (20) Sedaghat M., Naderi M., Zarei-Ghanavati M., Biomechanical parameters of the cornea after
321 collagen crosslinking measured by waveform analysis, J Cataract Refract Surg, 2010, 36: 1728-1731

322 (21) Wang H., Prendiville P.L., McDonnell P.J., Chang W.V., An ultrasonic technique for the
323 measurement fo the elastic moduli of human cornea, Journal of Biomechanics, 1996, 29(12): 1633-
324 1636

325 (22) Raiskup-Wolf F., Hoyer A., Spoerl E., Pillunat L.E., Collagen crosslinking with riboflavin and
326 ultraviolet-A light in keratoconus: Long-term results, Journal of Cataract & Refractive Surgery, 2008,
327 34(5): 796–801

(23) Hennighausen H., Feldman S.T., Bille J.F., McCulloch A.D., Anterior-Posterior Strain Variation in Normally Hydrated and Swollen Rabbit Cornea, Invest Othalmol Vis Sci, 1998, 39(2): 253-262

(24) Bueno J.M., Gualda E.J., Giakoumaki A., Pérez-Merino P., Marcos S., Artal P., Multiphoton microscopy of ex vivo corneas after collagen cross-linking, Invest Opthtalm Vis Sci, 2011, 52(8): 5325-5331

Figures:

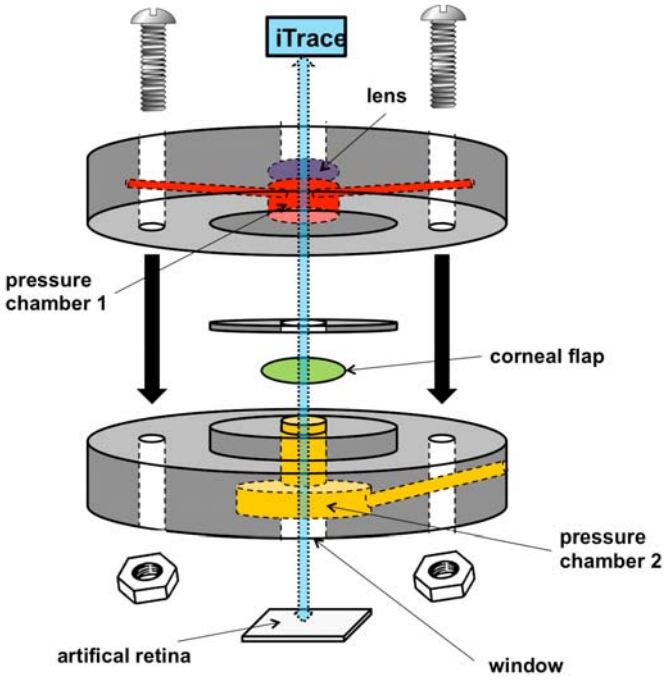

Figure 1. Flap mounting.

Figure 2. Measurement set-up.

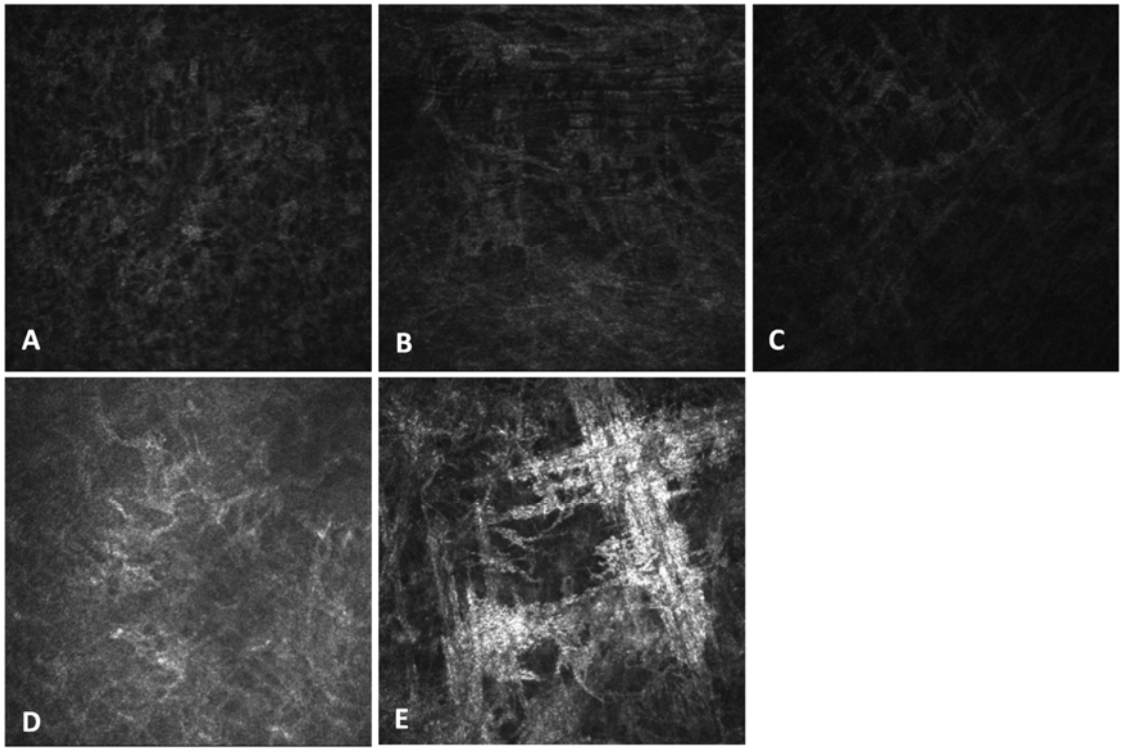

Figure 3. Confocal microscopy images comparing the mid stroma (about 130 µm depth) in three conditions (rabbits): (A) virgin cornea, (B) riboflavin instillation, (C) immediately post CXL, (D) one day post cxl, (E) one-month post-CXL.

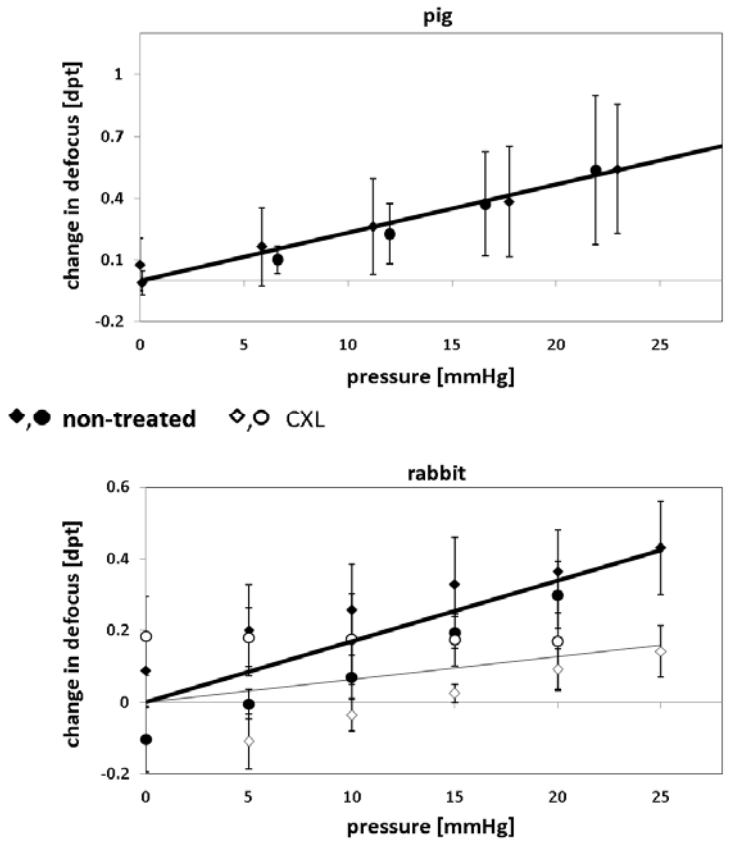

Figure 4. Changes in defocus as a function of pressure on the flap in (A) pig eyes and (B) rabbit eyes (non-treated versus CXL). Diamonds stand for pressure increase, and circles for pressure decrease. Open symbols represent cross-linked flaps and closed symbols non-treated flaps.

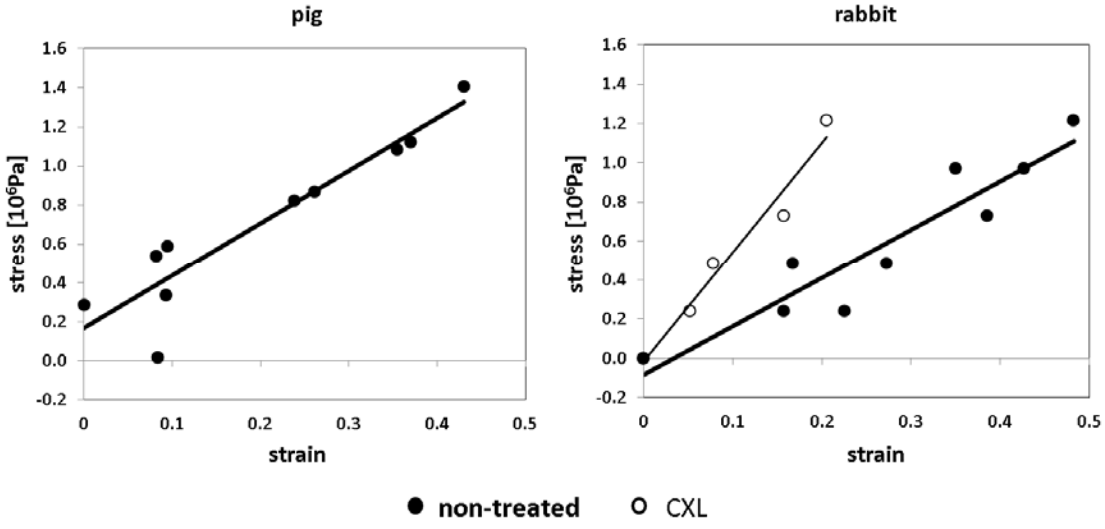

364 **Figure 5.** Stress-strain diagrams in (A) pig eyes and (B) rabbit eyes (non-treated and CXL). The Young
365 modulus was estimated from the slope of the linear trend lines of the average data from the loading
366 and unloading cycle. Open circles represent cross-linked flaps and closed circles non-treated flaps.